NOTES 13

SQUEEZE FILM DAMPERS: OPERATION, MODELS AND TECHNICAL ISSUES

Squeeze film bearing dampers are lubricated elements providing viscous damping in mechanical systems. Squeeze film dampers in rotating machinery provide structural isolation, reduce the amplitudes of rotor response to imbalance, and in some instances, assist to suppress rotordynamic instability.

Background

The most commonly recurring problems in rotordynamics are excessive steady state synchronous vibration levels and subsynchronous rotor instabilities. The first problem may be reduced by improved balancing, or by introducing modifications into the rotor-bearing system to move the system critical speeds out of the operating range, or by introducing external damping to limit peak amplitudes at traversed critical speeds. Subsynchronous rotor instabilities may be avoided by eliminating the instability mechanism, by rising the natural frequency of the rotor-bearing system as high as possible, or by introducing damping to increase the onset rotor speed of instability [Vance 1988, Childs 1993].

Lightweight, high performance engines exhibit a trend towards increased flexibility leading to a high sensitivity to imbalance with large vibration levels and reduced reliability. Squeeze film dampers (SFDs) are essential components of high-speed turbomachinery since they offer the unique advantages of dissipation of vibration energy and isolation of structural components, as well as the capability to improve the dynamic stability characteristics of inherently unstable rotor-bearing systems. SFDs are used primarily in aircraft jet engines to provide viscous damping to rolling element bearings which themselves have little or no damping. One other important application is related to high performance compressor units where SFDs are installed in series with tilting pad bearings to reduce (soften) bearing support stiffness while providing additional damping as a safety mechanism to prevent rotordynamic instabilities. In addition, in geared compressors, the SFD assists to reduce and isolate multiple frequency excitations transmitted through the bull gear, for example. [San Andrés, 2002].

Zeidan et al. [1996] give a history of the SFD in jet engines and detail design practices for successful SFD operation in commercial turbomachinery. Adilleta and Della Pietra [2002] provide a comprehensive review of the relevant analytical and experimental work conducted on SFDs. San Andrés and Delgado [2007] discuss more recent SFD experimental research and present a mechanically sealed SFD impervious to air entrainment.

In spite of the many successful applications, industry often recognizes that the design of SFDs is based on overly simplified predictive models that either fail to incorporate or simply neglect unique features (structural and fluidic) that affect the damper dynamic force performance. Actual damper performance can range from erratic to non-functioning depending on the operating conditions. Issues such as lubricant cavitation or air entrainment are of fundamental interest [San Andrés and Diaz,

2003].

Application fundamentals

Figure 1 shows a typical SFD configuration consisting of an inner nonrotating journal and a stationary outer bearing, both nearly equal in diameter. The journal is mounted on the external race of a rolling element bearing and prevented from spinning with loose pins or a squirrel cage that provides a centering elastic mechanism. The annular squeeze film, typically less than 0.250 mm, between the journal and housing is filled with a lubricant provided as a splash from the rolling element bearing lubrication system or by a dedicated pressurized delivery. In operation, as the journal moves due to dynamic forces acting on the system, the fluid is displaced to accommodate these motions. As a result, hydrodynamic squeeze film pressures exert reaction forces on the journal and provide for a mechanism to attenuate transmitted forces and to reduce the rotor amplitude of motion.

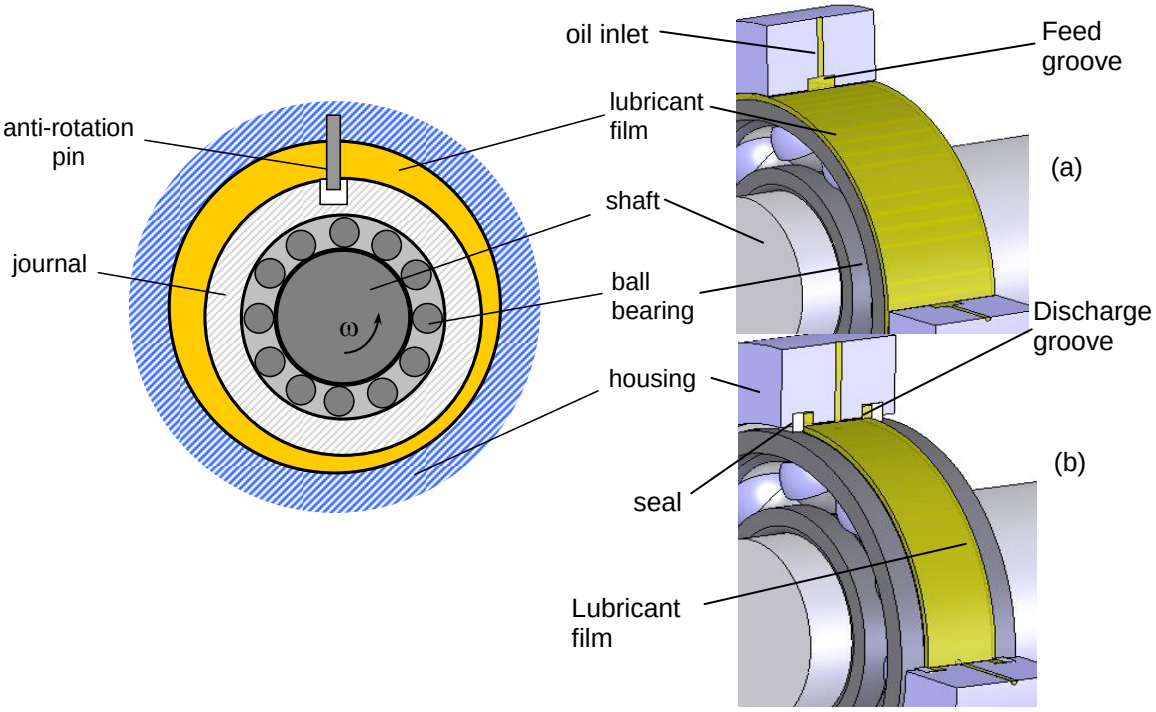

Fig 1. Squeeze film damper (SFD) configuration. a) SFD with central feed groove. b) SFD with end grooves and seals [1]

Figure 2 shows conceptual views of intershaft dampers for multiple-spool gas turbine engines. These dampers are subject to whirl motions resulting from the combined imbalance response of both low speed (LS) and high speed (HS) rotors. Most SFDs in US aircraft engines incorporate the arrangements in Figure 2(a & b) where the journal (and rolling element bearing) is elastically supported, and the bearing is rigidly attached to the engine frame. The (soft) spring support and squeeze film damper "see" the same deflections though the dynamic loads divide unequally between them.

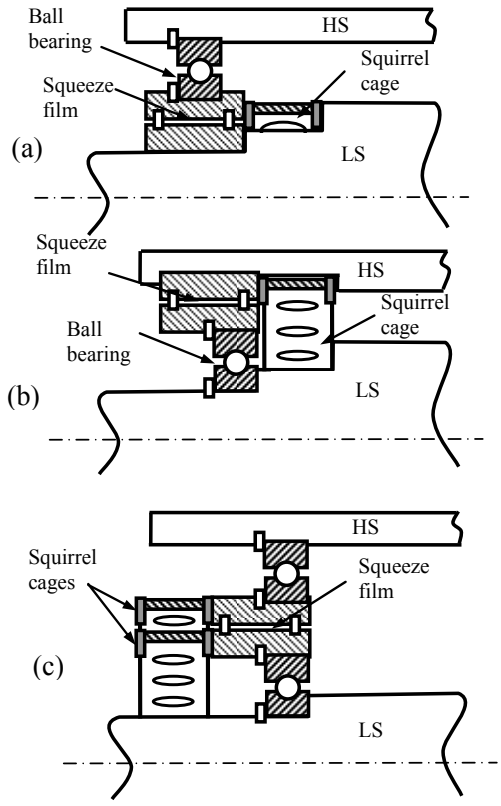

Fig. 2 Schematic views of intershaft damper configurations: a) squeeze film rotates with low speed (LS) rotor, b) Squeeze film rotates with high speed (HS) rotor, c) double ball bearing-squirrel cage design

Dampers in jet engines operate with low values of external pressurization (2 or 3 bar max.) to avoid excessive weight and volume in the lubrication system. Note also that most aircraft engines do not use any type of hydrodynamic journal bearings to avoid the risk of fluid film bearing induced instabilities. (However, in some dual shaft jet engines, the inter-spool fluid film bearing, shown in Figure 2a, is known to be a source of such instabilities).

The amount of damping produced is the critical design consideration. If damping is too large, the SFD acts as a rigid constraint to the rotor-bearing system with large forces transmitted to the supporting structure. If damping is too light, the damper is ineffective and likely to permit large amplitudes of vibratory motion with likely subsynchronous motions. Note also that a damping element to be effective needs to be "soft", thus allowing for motion at the location of the support, in particular for the modes of vibration of interest.

The damper geometry (length, diameter and clearance), operating speed and fluid properties (density and viscosity) determine, on first instance, the dynamic forced performance of *SFDs*. However, there are other important considerations that ultimately determine an appropriate operation.

The relevant issues are:

a) kinematics of journal (tied to rotor system and acting forces)
b) level of supply pressure for adequate flow rate and cooling,
c) feeding and end sealing mechanisms,
d) fluid inertia effects,
e) type of lubricant dynamic cavitation (vapor or gaseous) or air ingestion and entrapment.

Models for SFD dynamic forced performance

Most dampers in practice are of short axial length, *L/D < 0.50,* and accommodate some type of end seals to increase their damping capability. SFDs include additional features such as high resistance orifices for pressure delivery and discharge and/or deep grooves acting as flow sources or sinks of uniform pressure.

Squeeze film damper reaction forces and force coefficients are conveniently divided into two major types related to the specific journal center kinematics. For imbalance response analyses, SFD forces are obtained under the assumption of circular centered orbits. The model is applicable when the rotor traverses a critical speed, for example, where the imbalance force induces large amplitude orbital motions as the system may have little damping. On the other hand, for rotordynamic critical speed and stability analyses, SFD force coefficients are obtained for small amplitude journal center motions about a static (equilibrium) position. Only recently, computational tools analyze rotor-bearing system transient response events by considering the instantaneous SFD reaction forces as a function of the time varying journal kinematics that satisfy the equations of motion of the rotating system.

Figure 3 depicts a schematic view of a journal whirling within its bearing of radius *R (* ½ diameter *D)* and length *L*. Lubricant of density ρ and viscosity μ fills the radial clearance *c* between the bearing and its journal. The film thickness *h* is squeezed as the journal whirls and displaces fluid. The film thickness equals

$$h = c + \left(e_{X_o} + \Delta e_X(t)\right)\cos\left(\Theta\right) + \left(e_{Y_o} + \Delta e_Y(t)\right)\sin\left(\Theta\right) \qquad (1)$$

where $\left(e_{X_o},\, e_{Y_o}\right)$ and $\left(\Delta e_X(t),\, \Delta e_Y(t)\right)$ denote the static and dynamic components of journal motion, respectively. In operation, the dynamic journal motions coincide with the rotor speed for synchronous excitation from rotor imbalance, for example.

Unlike in conventional oil lubricated journal bearings, fluid inertia affects the performance of SFDs due to their typically larger clearances and operation at high frequencies. The squeeze film Reynolds number $\mathrm{Re}_s = \left(\rho\,\omega\,c^2\right)/\mu$ ranges from one to 50 in most practical applications. Fluid inertia effects are relevant in dampers with large clearances, using light viscous lubricants and operating at high frequencies (well above 10,000 rpm). In general, large clearance SFDs generate significant direct added mass coefficients that may lower significantly the critical speeds of compact rotating machinery, as in some small jet engine applications.

Considering **temporal fluid inertia** effects **only**, the equation governing the generation of the dynamic pressure field P is

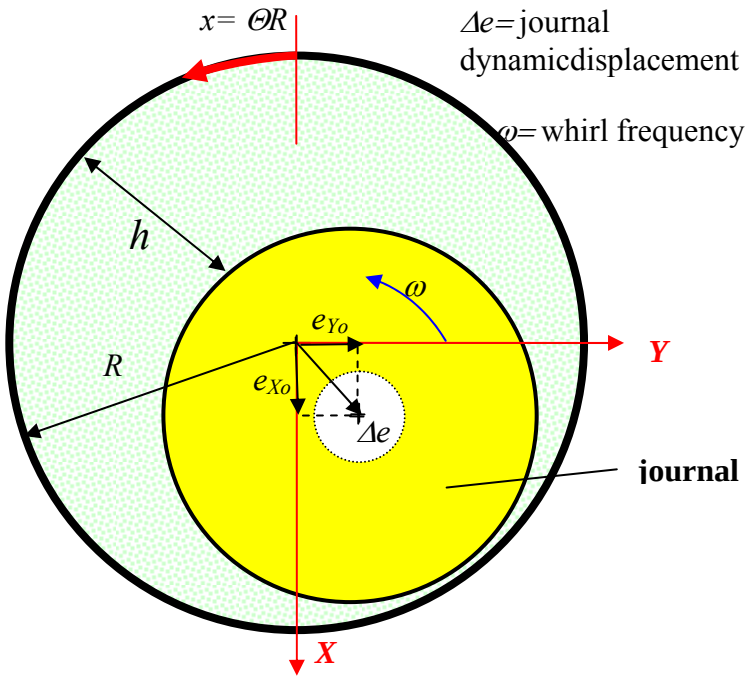

Fig. 3 View of whirling journal and coordinate system for analysis

$$\frac{\partial}{R\partial\Theta}\left(h^3\frac{\partial P}{R\partial\Theta}\right)+\frac{\partial}{\partial z}\left(h^3\frac{\partial P}{\partial z}\right)=12\,\mu\frac{\partial h}{\partial t}+\left(\rho h^2\right)\frac{\partial^2 h}{\partial t^2} \qquad (2)$$

Numerical solutions to Eqn. (2) with specific boundary conditions and accounting for lubricant cavitation (vapor or gas) are readily available [San Andrés, 2002]. Detailed physics based solutions modeling air ingestion and entrapment are yet to appear. The phenomenon is exceedingly complex, only understood in a time ensemble averaged manner, as described by San Andrés and Diaz [2003].

SFD rotordynamic force coefficients

SFD reaction forces due to small amplitude journal center motions about a static eccentric or off-centered position $\left(e_{X_o}=e_S,\, e_{Y_o}=0\right)$, as shown in Fig. 4, are of importance in the evaluation of critical speeds and stability of rotor-bearing systems mounted on dampers with soft or no centering springs. The damper forces are represented in the linearized form

$$\begin{bmatrix} F_X \\ F_Y \end{bmatrix} = -\begin{bmatrix} C_{XX} & C_{XY} \\ C_{YX} & C_{YY} \end{bmatrix}\begin{bmatrix} V_X \\ V_Y \end{bmatrix} - \begin{bmatrix} M_{XX} & M_{XY} \\ M_{YX} & M_{YY} \end{bmatrix}\begin{bmatrix} A_X \\ A_Y \end{bmatrix} \tag{3}$$

where (V_X, V_Y) and (A_X, A_Y) are the instantaneous journal center velocities and accelerations in the X and Y directions, respectively. $\left(C_{\alpha\beta}, M_{\alpha\beta}\right)_{\alpha,\beta=X,Y}$ are the damping and inertia force coefficients, respectively. Recall that a SFD does not produce direct stiffnesses, i.e. without journal spinning, a damper cannot generate film pressures given a journal static displacement.

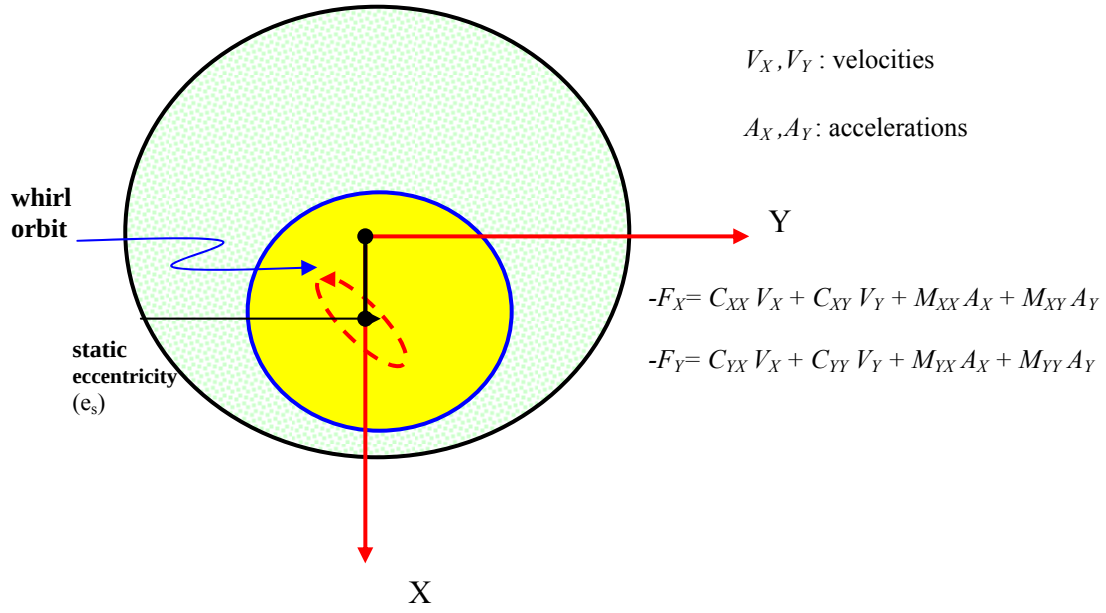

Fig. 4. SFD model: small amplitude journal motions about an static off-centered position

Table 1 shows formulas for the linearized force coefficients of a short length, open ends SFD. The coefficients are nonlinear functions of the static journal eccentricity ratio $(\varepsilon = e_S/c)$. The fluid inertia or added mass coefficients are strictly valid for small to moderate squeeze film Reynolds numbers, $\mathrm{Re}_s = \left(\rho \omega c^2\right)/\mu < 10$.

Table 1. Linearized force coefficients for open ends SFD
(small amplitude motions about a journal **off-center static** position $\varepsilon = e_y/c$)

Full film model (No cavitation)	**π-Film Model (Cavitated)**
$C_{XX} = \mu D \left(\frac{L}{c}\right)^3 \frac{\pi\left(1 + 2\varepsilon^2\right)}{2\left(1 - \varepsilon^2\right)^2}$	$C_{XX} = \mu D \left(\frac{L}{c}\right)^3 \frac{\pi}{2} \frac{\left[3\varepsilon + i \frac{\left(1 + 2\varepsilon^2\right)}{2}\right]}{2\left(1 - \varepsilon^2\right)^2}$
$C_{XY} = 0$	$C_{XY} = \mu D \left(\frac{L}{c}\right)^3 \frac{\varepsilon}{\left(1 - \varepsilon^2\right)^2}$
$C_{YY} = \mu D \left(\frac{L}{c}\right)^3 \frac{\pi}{2\left(1 - \varepsilon^2\right)^{3/2}}$	$C_{YY} = \mu D \left(\frac{L}{c}\right)^3 \frac{\pi}{4\left(1 - \varepsilon^2\right)^{3/2}}$
$C_{YX} = 0$	$C_{YX} = 0$
$M_{XX} = \rho D \left(\frac{L^3}{c}\right) \frac{\alpha\pi\left[1 - \left(1 - \varepsilon^2\right)^{1/2}\right]}{12\,\varepsilon^2\left(1 - \varepsilon^2\right)^{1/2}}$	$M_{XX} = \rho D \left(\frac{L^3}{c}\right) \frac{\alpha\,(i - \pi - 2\varepsilon)}{24\,\varepsilon^2}$
$M_{XY} = 0$	$M_{XY} = \rho D \left(\frac{L^3}{c}\right) \frac{\alpha\left[\ln\left\{\frac{(1 - \varepsilon)}{(1 + \varepsilon)}\right\} - 2\varepsilon\right]}{24\,\varepsilon^2}$
$M_{YY} = \rho D \left(\frac{L^3}{c}\right) \frac{\alpha\ \pi\left[1 - \left(1 - \varepsilon^2\right)^{1/2}\right]}{12\,\varepsilon^2}$	$M_{YY} = \rho D \left(\frac{L^3}{c}\right) \frac{\alpha\ \pi\left[1 - \left(1 - \varepsilon^2\right)^{1/2}\right]}{24\,\varepsilon^2}$
$M_{YX} = 0$	$M_{YX} = 0$

$i = \frac{2\cos(-\varepsilon)}{\left(1 - \varepsilon^2\right)^{1/2}}$, and α = 1.2-1.0 for small to moderately large squeeze film Reynolds numbers (Re_s < 50). Note that the coefficients C_{YX} and M_{YX} are nil.

For an open ends damper with L=63.5 mm, D=127 mm, c=0.137 mm and a light oil (μ= 2.14 10^{-3} Pa.s, ρ=785 kg/m^3), the graphs below depict the damping and inertia force coefficients derived for small amplitude motions about a static eccentric position (e_X). Note that L/D=0.5, i.e., the geometry does not represent strictly a short length damper. Realize that $C_{XX} > C_{YY}$, $M_{XX} > M_{YY}$; $C_{XY} = C_{YX}$=0, $M_{XY} = M_{YX}$=0. Both damping and inertia force coefficients are nonlinear, growing rapidly with the (static) eccentricity (e_X/c). Most importantly, the added mass coefficients are large in magnitude; M_{XX}. M_{YY} >~ 24.4 kg. Consider that the mass of fluid in the annular region is ($\rho\pi DLc$)=2.72 gram!

Force coefficients for the π-film (cavitated) damper are not shown. The author believes that these force coefficients are not usually apparent since for (very) small amplitude journal motions, oil

cavitation will not occur.

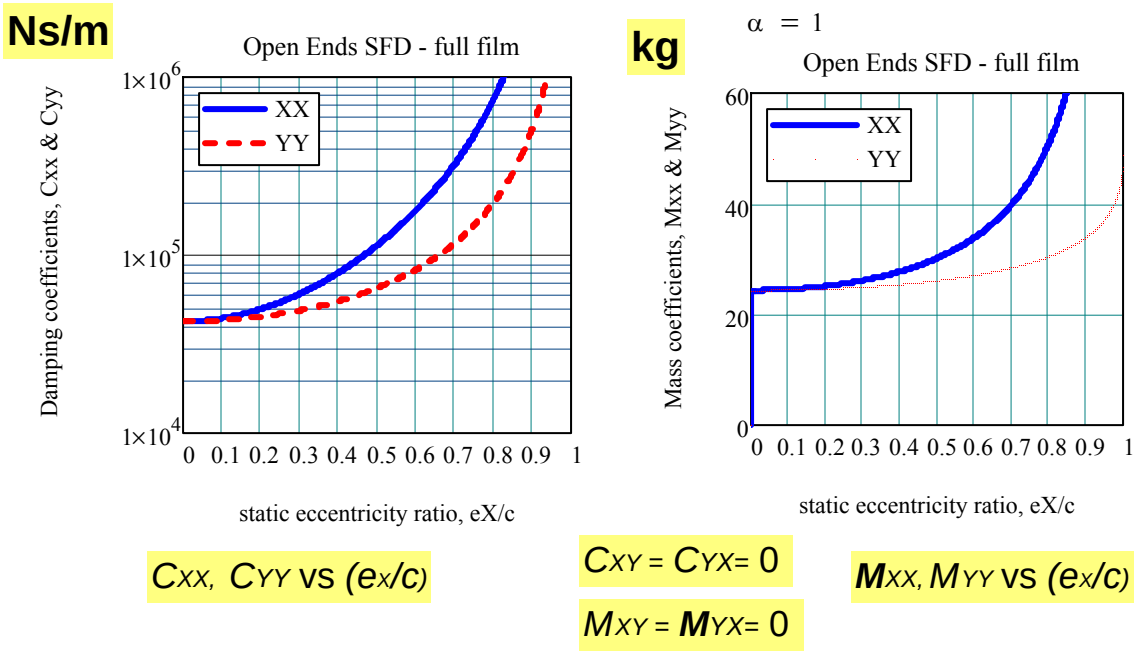

Fig. XX. Example: squeeze film damping and inertia coefficients for small amplitude motions about an off-centered journal static position (full film model)

SFD force coefficients for circular centered orbits

Figure 5 shows a SFD journal describing circular centered orbits of amplitude *(e)* and whirl frequency *(ω)*. The damper generates a constant reaction film force in a reference frame rotating with frequency ω. The radial (F_r) and tangential (F_t) components of the damper reaction force are

$$F_r = -\{C_{rt}\, V_t + M_{rr}\, A_r\}; \quad F_t = -\{C_{tt}\, V_t + M_{tr}\, A_r\} \tag{4}$$

where $V_t = e\omega$ and $A_r = -e\omega^2$ are the journal center tangential speed and radial acceleration, respectively. (C_{tt}, C_{rt}) denote the direct and cross-coupled viscous damping coefficients, and (M_{rr}, M_{tr}) are fluid inertia force coefficients, respectively. Recall that SFDs do not generate stiffness coefficients, i.e. reaction forces due to static journal displacements. The archival literature misleads the designer when referring to a damper direct radial stiffness, $K_{rr} = C_{rt}\, \omega$, that is frequency dependent.

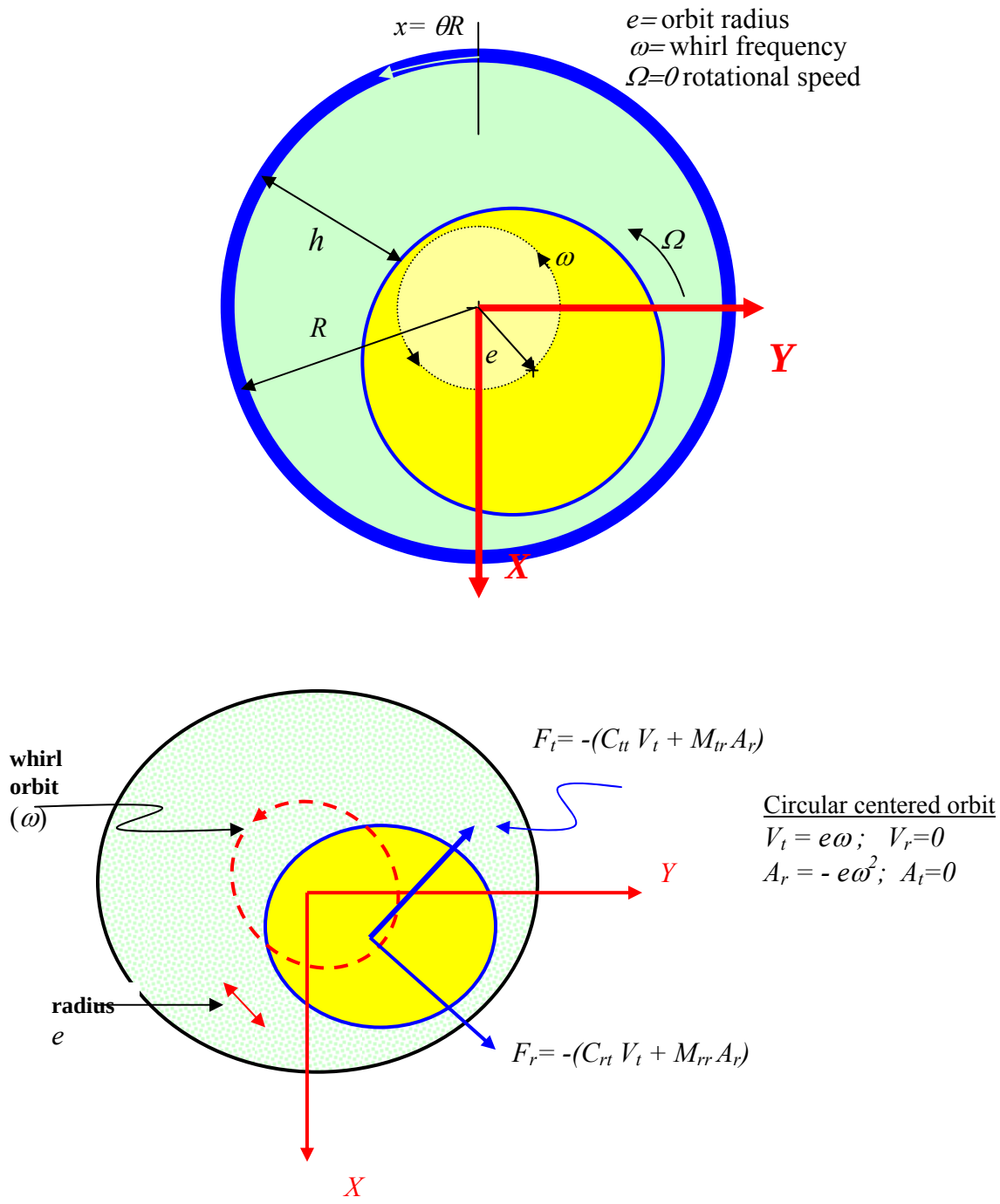

Fig. 5 SFD model: circular centered orbit with radius *e*

For the short-length open ends *SFD* model, the force coefficients using the rather simplistic π-film assumption (i.e. half the damper circumference develops film cavitation) are [Vance 1988]

$$C_{tt} = \frac{\pi \mu D}{4\left(1-\varepsilon^2\right)^{3/2}}\left(\frac{L}{c}\right)^3 ;\; C_{rt} = \frac{\mu\, \varepsilon\, D}{\left(1-\varepsilon^2\right)^2}\left(\frac{L}{c}\right)^3 \tag{5}$$

$$M_{rr} = \frac{\pi \rho D}{24}\left(\frac{L^3}{c}\right)\left[1-2\left(1-\varepsilon^2\right)^{1/2}\right]\left\{\frac{\left(1-\varepsilon^2\right)^{1/2}-1}{\varepsilon^2\left(1-\varepsilon^2\right)^{1/2}}\right\};$$
$$M_{tr} = -\frac{27}{140\,\varepsilon}\rho D\left(\frac{L^3}{c}\right)\left[2+\frac{1}{\varepsilon}\ln\left(\frac{1-\varepsilon}{1+\varepsilon}\right)\right] \tag{6}$$

where *(L, D, c)* denote the damper axial length, diameter and radial clearance, respectively, *(μ,ρ)* are the (effective) lubricant viscosity and density, and $\varepsilon = e/c$ is the dimensionless orbit radius. The orbit radius (*e)* should not be confused with the static journal offset displacement, null in this case. Note that the coefficients in Eqs. (5) and (6) are not strictly rotordynamic coefficients as their classical definition implies small amplitude motions (perturbations) about a journal equilibrium position.

The coefficients above are determined under the assumptions of an isoviscous and incompressible lubricant that is supplied with a low feed external pressure. Most importantly, the model assumes a squeeze film **fully submerged in a lubricant bath**. For the full film model (no oil cavitation), the direct coefficients *(C_{tt}, M_{rr})* are twice the values given by Eqs. (5) and (6), while the cross-coupled coefficients *(C_{rt}, M_{tr})* are null. The inertia force coefficients are strictly valid for small to moderate squeeze film Reynolds numbers, $\mathrm{Re}_s = \left(\rho\,\omega c^2\right)/\mu < 10$.

Figure 6 depicts the damping and inertia force coefficients for a short length, open ends SFD describing circular centered orbits *(CCOs)*. The damper length L=50 mm, c=0.080 mm, L/D=0.25, with lubricant viscosity and density (μ,ρ) equal to 20 centiPoise and 890 kg/m^3, respectively. The predicted force coefficients are highly nonlinear functions of the orbit radius *(e)*. Note the large magnitudes of direct damping *(C_{tt})* even for the centered position (e=*0*). The rapid growth of the cross-coupled damping coefficient *(C_{rt})* is referred as a "stiffness hardening effect," and the culprit of severe nonlinear (multiple valued) rotor response accompanied with jump-phenomenon and orbit-instability. However, these effects, mostly predicted by overly simplified theoretical analyses, are hardly ever reported in practice. Note that air entrainment is most prevalent for large amplitude orbital motions *($e \to c$)* and high frequencies of operation, determining a damper forced response quite different from the one derived from the force coefficients shown in the Figure.

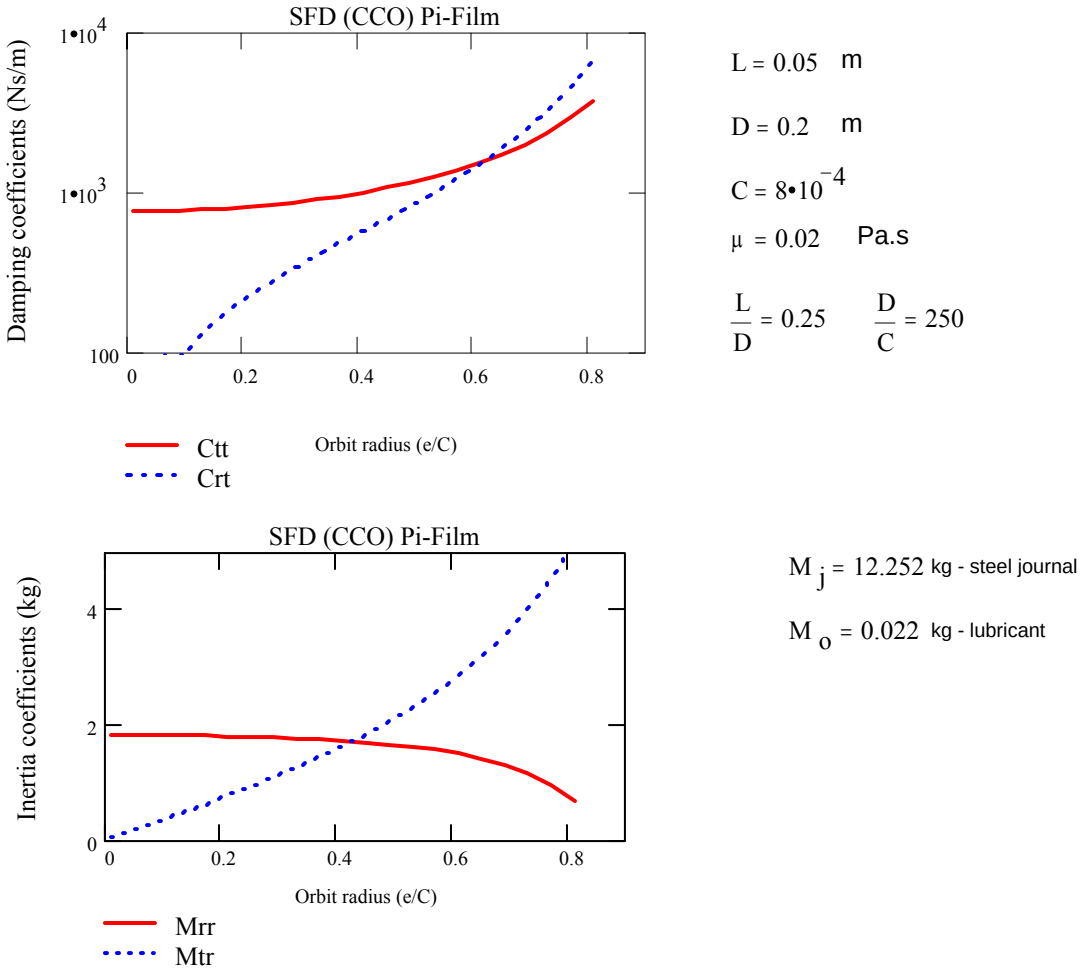

Fig. 6. Open ends SFD force coefficients for circular centered motions. (Short length π film model)

In actuality, stiffness hardening, K_{rr} >>0, is most likely due to contact and rubbing of the journal and bearing surfaces that may occur while a rotor traverses a critical speed with large orbital motions due to little damping or excessive rotor imbalance, for example. In these events, damper forces are negligible since the fluid film is probably ruptured with large amounts of air entrainment. Thus, predictions from a nonlinear rotor-SFD model based on the π-film short length SFD bear little relationship to reality.

The inertia force coefficients (M_{rr}, M_{rt}) have an effect on the system rotordynamic response, This is so in spite that the fluid mass, M_o, contained in the film $(\rho\pi DLc)$ is just a few grams. Note that the journal mass $(M_j=\rho_s\ \pi R^2 L)$ for a steel construction (ρ_s=7,800 kg/m^3) is 12.25 kg. Thus, the SFD added mass coefficients are of the same order of magnitude as the actual journal mass. Hence, fluid inertia in SFDs impacts the location of critical speeds in compact rotors operating at high rotational speeds.

For small amplitude motions (orbit radius $e/c < 0.25$), the SFD force coefficients in a full film, open ends SFD are [Reinhhart and Lund (1975), San Andrés (1985)]. The formulas are applicable to finite length SFDs.

$$C_{XX} = C_{YY} = C_{tt} = 12\pi \frac{\mu R^3 L}{c^3} \left[1 - \frac{\tanh\left(L/D\right)}{\left(L/D\right)} \right]$$

$$M_{XX} = M_{XX} = M_{rr} = \pi \frac{\rho R^3 L}{c} \left[1 - \frac{\tanh\left(L/D\right)}{\left(L/D\right)} \right] \qquad (7)$$

Note that the damping coefficient is proportional to $1/c^3$ while the inertia coefficient varies with $1/c$. Most importantly, contrary to a too long mistakenly held assumption, the added mass coefficient is ever present; that is, it is a physical property of the mechanical system. Its influence on the dynamics of a rotor-bearing system, however, becomes dominant at high frequencies, i.e. when the rotor accelerations ($A_r = -e\omega^2$) are large. At these operating conditions, the inertia forces $|M_{rr}A_r|$ are of the same order or even larger than the viscous force $|C_{tt}V_t|$, where $V_t = e\omega$.

There is good correlation between test derived and predicted force coefficients for *SFDs* operating with circular centered orbits [San Andrés, 1996]. The test damping coefficients *(C_{tt}, C_{rt})* fall in between the π- and full-film predictions. At low frequencies, the cavitation zone does not extend over half the damper circumference, and thus the damping coefficients approach the full film predictions. On the other hand, as the whirl frequency increases so does the squeeze film pressure and the cavitation zone extends. The experimental values thus approach those derived for the π-film model. It is most important to note that the experiments were conducted in a damper fully submerged within a lubricant bath. The test rig had closed any path that would permit the natural ingestion and entrapment of air. This condition in practice is most difficult to achieve. San Andrés and Delgado 2007] present more recent SFD parameters agreeing well with predictions, in particular for added mass coefficients, see Figure 7.

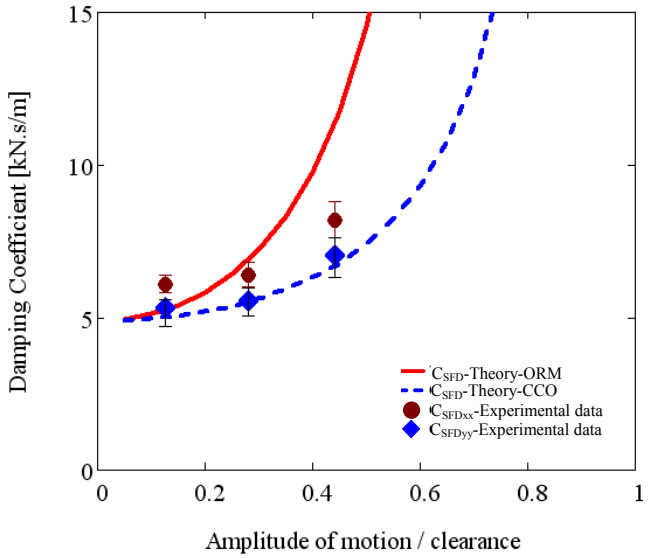

Fig. 7. Squeeze film damping coefficients identified from varying load amplitude - multi-frequency sine sweep forced excitations. Predictions for circular centered orbits (CCO) and radial motions about an off-centered journal static position (ORM).

The effect of air entrainment on squeeze film pressures and damper reaction forces has been thoroughly researched qualitatively and quantitatively in the last decade. San Andrés and Diaz [2003] report fundamental experimental results and advance an analytical model for thus most prevalent operating condition (see later for a further discussion on this issue).

A brief discussion follows on other physical and operating conditions that affect the performance of squeeze film dampers.

SFDs with feed grooves

Some dampers are designed with feed and discharge grooves to ensure a continuous flow of lubricant through the squeeze film lands, see Figure 8. A groove is thought to provide a uniform flow source with constant pressure around the bearing circumference. A central feed groove also divides the flow region into two separate squeeze film dampers working in parallel, i.e. the reaction forces from each land add.

For the central groove configuration, theory predicts forces about one-fourth less than that available for a damper with twice the land length and no groove. Experiments, however, demonstrate that grooved dampers generate much larger levels of forces that those derived from accepted theory. Large amplitude dynamic pressures are measured at the groove regions connecting the two squeeze film regions. Thus, a central groove does not isolate the adjacent film lands, but rather interacts with the squeeze film regions [Arauz et al., 1997, Childs et al. 2007].

Delgado [2008] presents a novel model for prediction of the forced response of grooved *SFDs* and grooved oil seal rings. The model includes fluid inertia and flow interactions at the groove-film land interface that amplify the generation of squeeze film pressures. Delgado's model predictions are in

excellent agreement with measured stiffness, damping and inertia force coefficients in oil seal rings with multiple cavities and in dampers with inlet and discharge deep grooves.

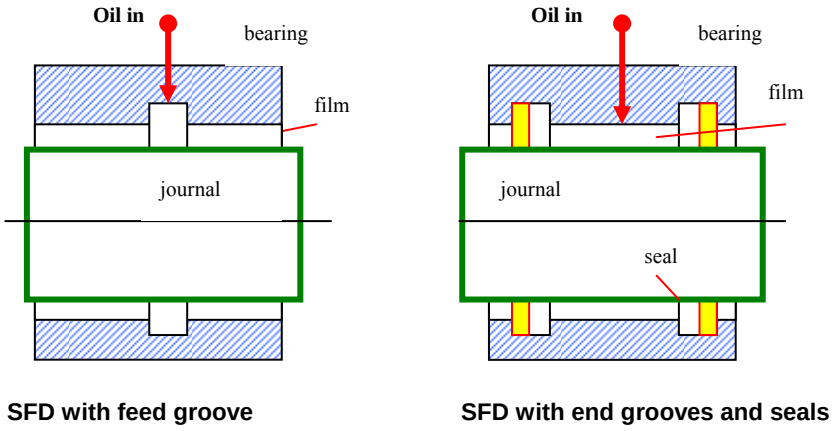

Fig. 8 SFD: grooved configurations

SFDs with end seals

SFDs usually incorporate some type of end seals to reduce the through flow and to amplify the viscous damping. The most common end seal configurations include O-rings, piston rings, and end plate (clearance gap) seals, as shown in Figure 9. Measurements and analysis show larger forces for the end-sealed condition, although the lubricant heats rapidly (lower viscosity) for designs with little through flows. The design of end seals is highly empirical and requires of "leakage correction factors" that can only be extracted from exhaustive experimentation. To date, only experience dictates the best type of sealing to be implemented.

SFDs in jet engine rotors incorporate piston rings as end seals. However, ring cocking and locking with a resulting excessive oil leakage is a pervasive problem. Implementing patented (proprietary) designs seems to resolve the reliability issue.

Many industrial compressor applications also implement dampers with O-ring end seals due to their simplicity and good sealing. However, these applications are restricted to low static loads and low temperatures. Material compatibility of the O-rings with the lubricant and gas external medium is a design consideration. Long-term relaxation and creep of the elastomeric O-rings, when supporting large static loads, is an issue usually overlooked that later can prove fatal.

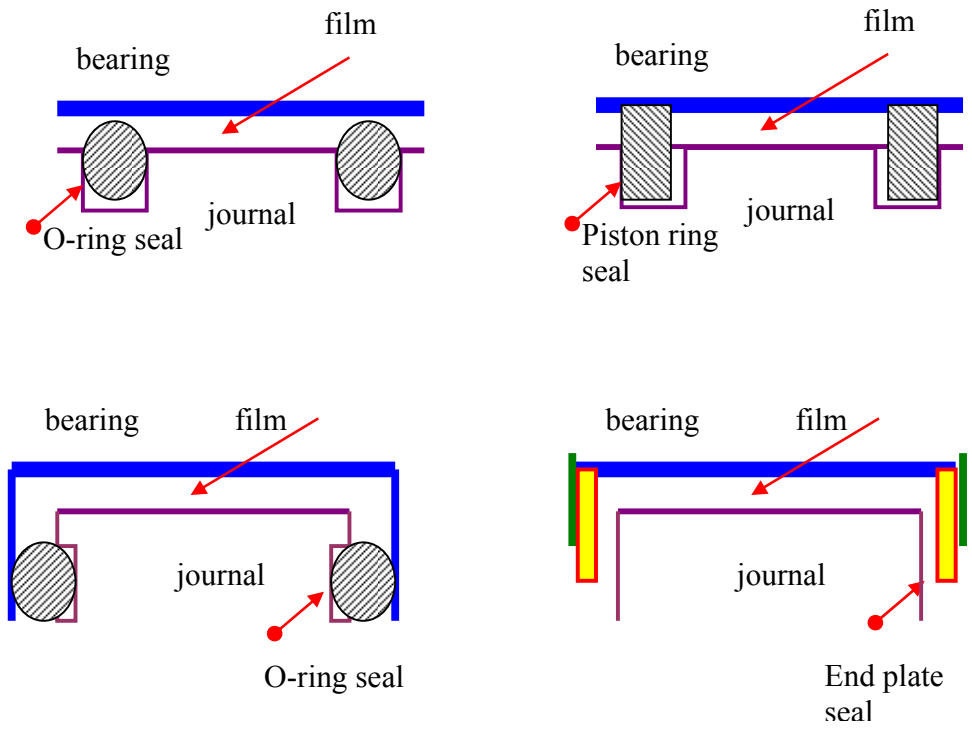

Fig. 9 SFD: types on end seals

San Andrés and Delgado [2007] detail parameter identification measurements conducted on a squeeze film damper (SFD) featuring a non-rotating mechanical seal that effectively eliminates lubricant side leakage. The SFD-seal arrangement generates dissipative forces due to viscous and dry-friction effects from the lubricant film and surfaces in contact. The identified system damping coefficients are frequency and motion amplitude dependent due to the dry friction interaction at the mechanical seal interface. Squeeze film force coefficients, damping and added mass, are in agreement with simple predictive formulas for an uncavitated lubricant condition and are similar for both flow restrictor sizes. The SFD-mechanical seal arrangement effectively prevents air ingestion and entrapment and generates predicable force coefficients for the range of frequencies tested.

Lubricant cavitation vs. air ingestion in squeeze film dampers

Zeidan et al. [1996] identify SFD operation with distinct types of dynamic fluid cavitation (vapor or gas) and a regime due to air ingestion and entrapment. The appearance of a particular condition depends on the damper type (sealed or open to ambient), magnitude of supply pressure and flow rate, whirl frequency, and magnitude of dynamic load producing (small or large) journal excursions within the film clearance.

Gas cavitation following the journal motion appears in ventilated (open ends) SFDs operating at low frequencies and with small to moderate journal amplitude motions. A well defined cavitation bubble containing the release of dissolved gas in the lubricant or air entrained from the vented sides follows the whirling motion of the journal; i.e. the cavitation zone appears steady in a rotating frame. The traveling gas bubble appears not to affect the generation of the squeeze film pressure in the full film zone. The persistence of this cavitation regime upon

reaching steady operating conditions (high frequencies) in an aircraft application is remote.

Lubricant vapor cavitation appears in dampers with tight end seals that prevent entrainment of the external gas media and for operation with a sufficiently large supply pressure. In this last case, the through oil flow also prevents the ingestion of air. Furthermore, the lubricant must be relatively free of dissolved gases such as air, a condition not readily found in practice.

Figure 10 depicts a measured dynamic film pressure versus time in a damper operating with lubricant vapor cavitation. The experiment illustrates the variation of dynamic squeeze film pressure and gap (film thickness) for five periods of journal orbital motion. The whirl frequency and centered journal orbital amplitude equal 75 Hz and 0.180 mm, respectively. The damper radial clearance is 0.343 mm. The damper is fully flooded in a lubricant bath; the supply pressure is 1.45 bar and the discharge is at atmospheric pressure. Note that the pressure profile is smooth and shows nearly identical shapes for each consecutive period of motion. A (flat) constant pressure zone develops at nearly zero absolute pressure, and it corresponds to the rupture of the film and formation of a vapor filled cavity. The cavity appears only during that portion of the journal motion cycle where the film gap increases. The vapor bubble collapses immediately as the local pressure rises above the lubricant vapor pressure. In general, correlations of measured pressures and vapor cavitation extent with predictions based on traditional film rupture models are satisfactory. [Diaz and San Andrés, 1999].

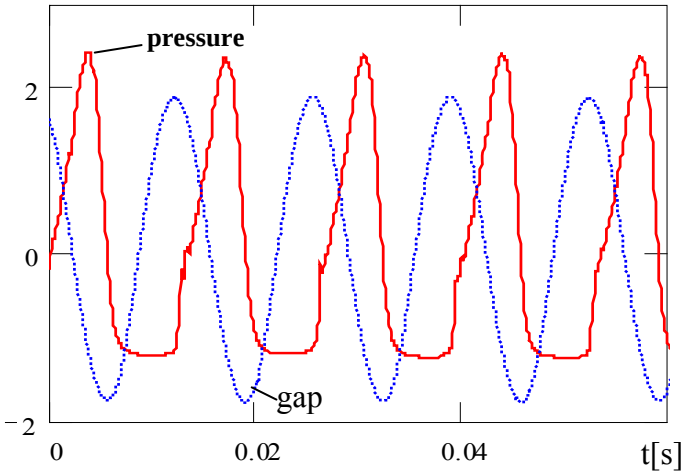

Fig. 10 Dynamic film pressure (bar) and local film gap (mm x 10) in a flooded SFD leading to vapor cavitation

Air ingestion and entrapment appear in vented dampers operating at high frequencies and with low magnitudes of supply (feed) pressure, i.e. small throughout flow rates. Figure 11 depicts the measured dynamic film pressure versus time in a SFD with air entrainment. The

operating conditions are identical to those for the measurements depicted in Figure 10, except that the damper is open to ambient conditions, i.e. not submerged in an oil bath. A suction pressure draws air into the thin film at the locations where the local film gap is increasing. The cyclic fluid motion leads to air entrapment, with bubbles remaining in the zones of dynamic pressure generation above ambient. Air ingestion leads to the formation of intermittent air fingering surrounded by liquid striations, see Figure 12 for vivid details. These islands of air may shrink, break up into smaller zones, or diffuse within the lubricant. The size and concentration of the ingested air fingers depend on the journal whirl frequency and amplitude and the flow rate. The fluid at the damper discharge is cloudy and foamy. [San Andrés and Diaz, 2003]

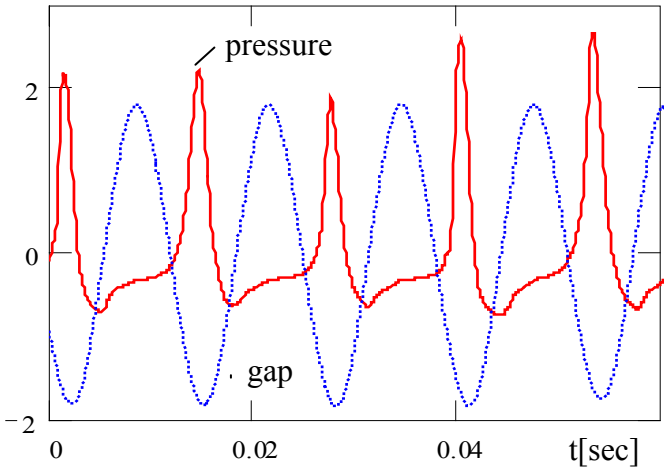

Fig. 11. Dynamic film pressures (bar) and local film gap (mm x 10) in a SFD operating with air entrainment

The dynamic pressures with air entrainment, Figure 11, show important differences when compared to those pressures induced by lubricant vapor cavitation, Figure 10. In the case of air ingestion, the squeeze film pressures differ markedly from one period to the next, and with peak pressures showing large variations. Furthermore, the pressure flat zone is nearly at ambient pressure. Note that subambient film pressures are also generated.

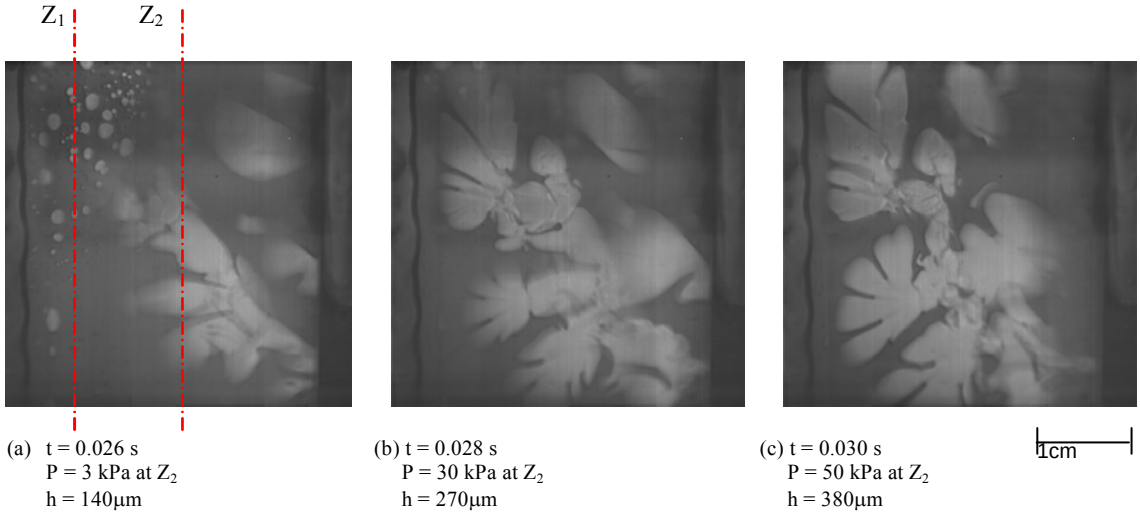

Fig. 12 Photographs of SFD flow field with air ingestion and entrapment. Tests with whirl frequency at 25 Hz and feed pressure 1.93 bar. Elapsed time for photographs is 2 ms (Period = 40 ms).

Inevitably, the vast majority of SFDs operate with foam-like fluids considering the low values of pressure supply (small flow rate), large damper clearances, and high operating whirl frequencies. Of course, mixed operation regimes can also occur in practice. For instance, tightly sealed dampers may show both vapor and air entrainment type cavitation where gas bubbles may coexist around a large lubricant vapor bubble. Note that the entrapment of air delays the increase of film pressures since there is less liquid lubricant filling the damper clearance. Ultimately, operation at high frequencies leads to an increase in air ingestion, preventing any further oil vapor cavitation, and reducing considerably the forces available from the *SFD*.

Careful experimentation demonstrates that air ingestion and entrapment degrades considerably the forced response of open ends SFDs [San Andrés and Diaz, 2003]. A simple criterion gives the likelihood of air entrainment in a damper. A feed-squeeze flow parameter (γ) relates the lubricant supply flow rate Q_{oil} to the dynamic change in volume within the squeeze film gap, i.e.

$$\gamma = \frac{Q_{oil}}{\pi D L e \omega} \tag{7}$$

If γ>1 then no air entrainment occurs, i.e. the through flow is sufficient to fill the volume change caused by the journal whirl motion. On the other hand, air ingestion and entrapment will occur when γ<1. The lower the feed-squeeze parameter (γ), the more severe the degradation in damper forced performance. The experimental results advance an empirical correlation between γ and the amount of air entrained (volume concentration of air) in the lubricant, thus providing certainty in the modeling of the mixture. Note that Q_{oil} is proportional to the difference between lubricant supply pressure and discharge pressure and to the flow conductances in the film lands and through the feed ports. The flow conductances (~1/resistances) are a function of the damper clearance and feed characteristics, lubricant and mixture viscosities, etc. Thus, air entrainment is device dependent, and its severity increases with the amplitude and frequency of journal

motion. Air ingestion can be prevented by increasing the supply pressure (not practical) to ensure a sufficiently large through lubricant flow rate.

Modern squeeze film dampers

The basic design of SFDs changed little until the late 1990's when the novel wire-EDM processes allowed the construction of integral SFDs which offer distinct advantages such as reduced overall weight and length of the damper structure with less number of parts, accuracy of positioning (centering), and a split segment construction allowing easier assembly, inspection and retrofit than with any other type of damper.

Flexure pivot tilting pad bearings offer similar construction features while minimizing (assembly) stack up tolerances and avoiding pivot wear and fretting. These features are most important in aircraft engines where reduced weight and size are of utmost consideration. The integral damper, as shown in Figure 13, comprises of segmented pads instead of a fully cylindrical journal. Thin structured webs attach the inner and outer rings and perform the function of elastic supports. The thin gap between the pads and the outer ring forms the squeeze film lands. Each pad can be manufactured with a different clearance to counter the static deflection due to rotor weight. End seals restricting the axial flow through the film lands dampers provide the means to increase the damping coefficients by raising the hydrodynamic pressure in a pad film land. The series combination of a tilting pad bearing and a squeeze film damper has been implemented in numerous compressors to introduce flexibility and damping to the bearing support. The proper design of these two mechanical elements allows for the optimum damping coefficient at the bearing support and accurate relocation of the (rigid mode) rotor bearing system critical speeds away from the operating speed range. De Santiago et al. [1999] provide experimental verification and theoretical validations of the damping capability of sealed integral dampers and demonstrate the benefits of this novel technology for application in modern high performance turbomachinery.

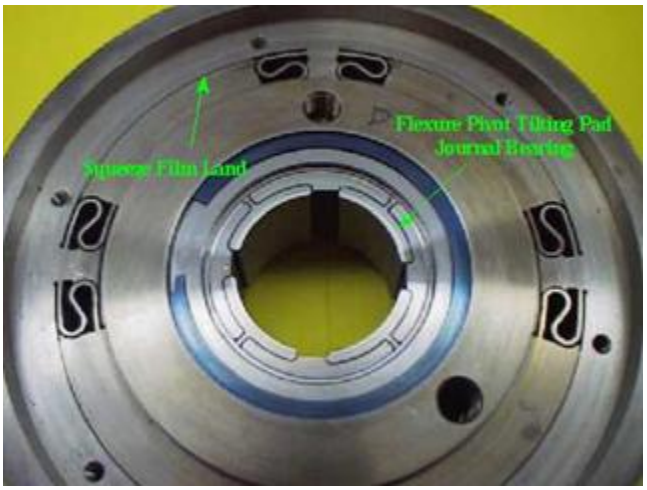

Fig. 13. Series integral SFD and flexure pivot tilting pad bearing

Closure

Decades of practice demonstrate that SFDs generate the required damping even when operating with persistent air entrainment. Damper support flexibility (structural stiffness) is the key parameter that allows the device intended operation in a practical application. Incidentally, the actual reduction of predicted damping at high frequencies (due to air ingestion, for example) is beneficial in rotor-bearing systems operating at supercritical speeds. However, the trend toward higher operating speeds and more stringent operating conditions demands of a reliable predictive physical model, experimentally verified.

Childs [1993] noted that, because of lubricant cavitation and unquantifiable air ingestion, correlation between theory and experiment is less compelling for SFDs than journal bearings. In practice *SFDs* operate with low magnitudes of oil feed pressure (5 bar max.) that generally do not prevent the lubricant in the fluid film lands from liquid vaporization or entrainment of external gaseous media into the film lands. Open-ends SFDs are prone to develop a flow regime where the ingestion of air leads to the formation of a *bubbly* lubricant. Actual practice demonstrates that air ingestion greatly affects the SFD dynamic forced response.

URL http://rotorlab.tamu.edu/TRIBGroup stores digital movies recorded in a transparent squeeze film damper while operating with air entrainment[1]. The movies vividly depict air ingestion and entrapment cycles with notable effects on the recorded squeeze film pressures and ensuing damper dynamic forced response.

Most (numerical) models for prediction of finite length SFD forced response assume lubricant vapor cavitation, i.e. an operating condition likely to be found with very tight end seals or when the damper is fully submerged in a lubricant bath. Understanding of air entrainment, a pervasive phenomenon in SFDs, has just begun.

References

Reinhardt, F., and Lund, J. W., "The Influence of Fluid Inertia on the Dynamic Properties of Journal Bearings," 1975, ASME J. Lubr. Technol., **97**(1), pp. 154-167.

San Andrés, L., 1985, "Effect of Fluid Inertia Effect on Squeeze Film Damper Force Response," Ph.D. Dissertation, December, Texas A&M University, College Station, TX

J. Vance, Rotordynamics of Turbomachinery, (1988), John Wiley and Sons, New York.

D. Childs, Turbomachinery Rotordynamics, (1993), John Wiley and Sons, New York

F. L. Zeidan, L. San Andrés and J. Vance, Design and Application of Squeeze Film Dampers in Rotating Machinery, Proceedings of the 25th Turbomachinery Symposium, (1996), Houston, TX, September, pp. 169-188.

L. Della Pietra and G. Adiletta, The Squeeze Film Damper over Four Decades of Investigations.

1 Funded by US National Science Foundation, 1996-2000

Part I: Characteristics and Operating Features, Shock Vib. Dig, (2002), **34**(1), pp. 3-26, Part II: Rotordynamic Analyses with Rigid and Flexible Rotors, Shock Vib. Dig., (2002), **34**(2), pp. 97-126.

L. San Andrés and A. Delgado, Identification of Force Coefficients in a Squeeze Film Damper with a Mechanical End Seal- Centered Circular Orbit Tests, (2007), ASME J. Tribol., **129**(3), pp. 660-668.

L. San Andrés and S. Diaz, Flow Visualization and Forces from a Squeeze Film Damper with Natural Air Entrainment, ASME J. Tribol., (2003), **125**, pp. 325-333.

L. San Andrés, Theoretical and Experimental Comparisons for Damping Coefficients of a Short Length Open-End Squeeze Film Damper, ASME Journal of Engineering for Gas Turbines and Power, (1996), **118**, pp. 810-815

G. Arauz and L. San Andrés, Experimental Force Response of a Grooved Squeeze Film Damper, Tribology International, (1997), **30,** pp. 77-86,.

D. W. Childs, M. Graviss and L.E. Rodriguez, The Influence of Groove Size on the Static and Rotordynamic Characteristics of Short, Laminar-Flow Annular Seals, ASME J. Tribol, (2007), **129**(2), 398-406.

A. Delgado, A Linear Fluid Inertia Model for Improved Prediction of Force Coefficients in Grooved Squeeze Film Dampers and Grooved Oil Seal Rings, (2008), Ph.D. Dissertation, Texas A&M University, College Station, TX.

O. De Santiago, L. San Andrés and J. Oliveras, Imbalance Response of a Rotor Supported on Open-Ends, Integral Squeeze Film Dampers, ASME Journal of Gas Turbines and Power, (1999), **121**(4), pp. 718-724, 1999.

Text books and summary papers

Childs, D., 1993, "Turbomachinery Rotordynamics," John Wiley & Sons, New York

Vance, J., 1988, "Rotordynamics of Turbomachinery," John Wiley and Sons, New York.

Zeidan, F., 1995, "Application of Squeeze Film Dampers", Turbomachinery International, Vol. 11, September/October, pp. 50-53.

Zeidan, F., L. San Andrés, and J. Vance, "Design and Application of Squeeze Film Dampers in Rotating Machinery," Proceedings of the 25th Turbomachinery Symposium, Turbomachinery Laboratory, Texas A&M University, September, pp. 169-188, 1996.

L. Della Pietra and G. Adiletta, The Squeeze Film Damper over Four Decades of Investigations. Part I: Characteristics and Operating Features, Shock Vib. Dig, (2002), **34**(1), pp. 3-26, Part II: Rotordynamic Analyses with Rigid and Flexible Rotors, Shock Vib. Dig., (2002), **34**(2), pp. 97-

126.

Historical papers

Cooper, S., 1963, "Preliminary Investigation of Oil Films for the Control of Vibration," Paper 28, Proceedings of the Lubrication and Wear Convention, Instn. Mech. Engrs., U.K.

Friedericy, J. A., Eppink, R. T., Liu, Y. N., and Cetiner, A., 1965, "An Investigation of the Behavior of Floating Ring Dampers and the Dynamics of Hypercritical Shafts on Flexible Supports," USAAML Technical Report 65-34, UVA Report No. CE-3340- 104-65U.

Parsons, R. H., 1936, "The Development of the Parsons Steam Turbine," Constable and Co. Ltd., London.

Visit URL: http://rotorlab.tamu.edu/TRIBGroup to learn more about a long-term SFD research project sponsored by industry and government. The site details the existing test rigs, experimental data and comparisons to model predictions. The site also provides a full list of technical reports and archival papers.